A kinetic model of dissolved air flotation including the effects of interparticle forces

D. M. Leppinen

ABSTRACT

This paper examines a mathematical model of the overall removal rate of particles during dissolved air flotation. It is shown that the particle capture efficiency for an isolated bubble–particle interaction can be calculated directly using a mathematical model provided the physicochemical properties of the bubble and particle are known. The mathematical model incorporates the exact hydrodynamics for an isolated bubble–particle interaction, including the influences of van der Waals forces and electrostatic forces. The mathematical model is used to determine how the overall flotation rate depends on bubble and particle size and on interparticle forces. It is shown that, if complete particle charge neutralisation can be achieved, then the overall rate of flotation can be enhanced by decreasing bubble sizes while increasing floc sizes.

Key words | adhesion efficiency, bubble–particle attachment, dissolved air flotation, flotation rate, interparticle forces, kinetics

D. M. Leppinen
Department of Applied Mathematics and Theoretical Physics,
University of Cambridge,
Silver Street,
Cambridge CB3 9EW,
UK
Tel: (+44) 1223 337744;
Fax: (+44) 1223 337918;
E-mail: *D.M.Leppinen@damtp.cam.ac.uk*

INTRODUCTION

Dissolved air flotation is a gravity assisted separation process in which air bubbles are used to remove solid particles from a liquid. In dissolved air flotation bubbles are typically 10–100 μm in diameter. They are generated by first saturating the water with air at high pressure, and then reducing the pressure so that the supersaturated dissolved air is forced out of solution in the form of microscopic bubbles. As the bubbles rise through the water column they interact with the suspended particles. If a bubble–particle interaction results in a collision and successful bubble–particle attachment, and if the resulting bubble–particle agglomerate is positively buoyant, then the bubble will carry the particle to the foam layer at the top of the flotation tank which can then subsequently be skimmed off. Flotation has been used extensively for mineral processing since the early 1900s, while the use of dissolved air flotation for potable water production dates from the 1970s (Zabel 1977). Dissolved air flotation has the advantage over the conventional technique of sedimentation of being able to efficiently remove low density flocs and algae which might otherwise cause filter blocking.

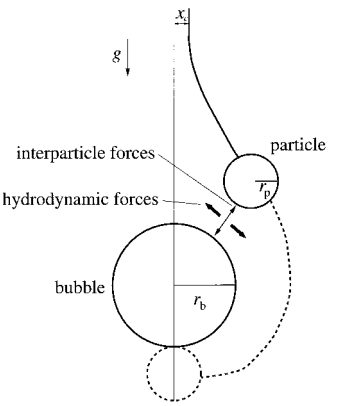

Figure 1 | The approach of a rising bubble and a falling particle indicating the influence of hydrodynamic forces and interparticle forces. The dashed line is the continuation of the particle trajectory indicating particle capture at the rear of the bubble.

The elementary act of flotation is the successful collision and attachment of a bubble and particle to form a positively buoyant bubble–particle agglomerate. Figure 1 shows a schematic of the interaction between a

rising bubble and a falling particle in an otherwise quiescent environment. The bubble and particle paths are vertical at large separation distances due to the force of gravity. At smaller separation distances however, hydrodynamic forces cause the bubble and particle to move horizontally away from each other. These hydrodynamic forces result from attempting to push fluid out of the gap between the bubble and the particle, with the forces increasing as the gap size decreases. In fact, in the absence of interparticle forces such as electrostatic forces or van der Waals forces (or in the case of sub-micron size particles, in the absence of Brownian motion), hydrodynamic forces will completely suppress collisions between bubbles and particles.

With reference to Figure 1, the removal efficiency for a single bubble–particle interaction can be defined as

$$E = \frac{x_c^2}{(r_p + r_b)^2} \tag{1}$$

where r_b is the bubble radius, r_p is the particle radius and x_c is the critical horizontal separation distance between the bubble and particle at a large distance upstream. If the initial horizontal separation distance between the bubble and particle is such that $x < x_c$, then the bubble and particle collide and successfully form a bubble–particle agglomerate. Experimentally it has been shown that the relative trajectories of particles around bubbles are influenced both by van der Waals forces and by electrostatic forces (Okada *et al*. 1990) while Collins & Jameson (1976, 1977) have shown that flotation removal rates are strongly dependent on the electrical properties of bubble and particle surfaces. Therefore it follows that the critical separation distance x_c will be a function of the relative strengths of the hydrodynamic and interparticle forces acting on the bubble and the particle.

The solid fractions encountered during the use of dissolved air flotation for potable water treatment is very small (with a suspended solids mass concentration of typically 10 mg ℓ^{-1} or less (Edzwald 1995)), and it is thus valid to model the removal of particles as a statistical two-body event involving the isolated interaction of a single particle and a single bubble. If n_p is the number of particles of radius r_p and $\dot{n}_b''$ is the number of air bubbles of radius r_b generated per unit time per unit area of the flotation test cell, then the rate of decrease of particles with time t is given by

$$\frac{dn_p}{dt} = -\pi(r_p + r_b)^2 E \dot{n}_b'' n_p \tag{2}$$

$= -$ (probability of a single bubble–particle interaction resulting in removal) $\times$ (the number of interactions per unit time).

If the removal efficiency E and the bubble flux $\dot{n}_b''$ are constant then Equation (2) can be integrated directly to give

$$n_p = n_p(0) e^{-Rt} \tag{3}$$

where $n_p(0)$ is the initial number of particles in the system and

$$R = \pi(r_p + r_b)^2 E \dot{n}_b'' \tag{4}$$

is the flotation rate constant. The situation modelled by Equations (2) and (3) is precisely that described by Pan *et al*. (1996) in their global model of flotation efficiency which they use to describe the removal of particles from a batch flotation test cell. Equation (2) assumes that a particle is removed from the system immediately after the successful formation of a positively buoyant bubble–particle agglomerate with no account being made for the finite rise time of the agglomerate to the top of the flotation test cell.

The removal efficiency in Equation (2) determines the rate of particle removal for fixed bubble and particle sizes and for fixed bubble flux. As noted above with reference to Figure 1, E is determined by the relative strength of hydrodynamic forces and interparticle forces. Malley & Edzwald (1991) have argued that E can by determined by the product

$$E = \eta_T \alpha_{pb} \tag{5}$$

where η_T is the total single collector efficiency for bubble–particle collisions and α_{pb} is the adhesion efficiency which represents the fraction of all successful

bubble–particle collisions which result in the successful formation of a bubble–particle agglomerate. Using simplified hydrodynamics (Yoon & Luttrell 1989) the single collector efficiency can be approximated by

$$\eta_T = \frac{3}{2}\left(\frac{r_p}{r_b}\right)^2 \tag{6}$$

and this result has been incorporated in many models of dissolved air flotation removal efficiency (e.g. Edzwald 1995; Liers *et al*. 1997; Bloom & Heindel 1997). The value of the adhesion efficiency depends on chemical pretreatment parameters such as the type of coagulant used, the coagulant dosage and pH. Bubble–particle adhesion is facilitated by the production of hydrophobic particles with neutral surface charge. As noted by Liers *et al*. (1997), the value of α_{pb} cannot be specified *a priori* for a given system: it must be determined empirically from the outcome of flotation experiments.

The purpose of this paper is to show that the removal efficiency E can be determined explicitly without introducing the concept of single collector efficiency and adhesion efficiency. Instead a mathematical model is employed which accounts for the exact hydrodynamics of the bubble–particle interaction and which incorporates the effects of interparticle forces. Using this model it will be shown that the rate of solids removal during dissolved air flotation can be optimised. This model requires the input of physicochemical properties of the bubble and particle which can either be measured using laboratory tests or estimated from results in the literature.

MATHEMATICAL FORMULATION

Flotation removal efficiency is modelled in this paper by examining the interaction between a rising bubble and a falling particle in an otherwise quiescent environment. The bubble is assumed to behave as a positively buoyant solid sphere with no surface mobility due to the presence of surfactants. Due to the small size of the bubbles used in dissolved air flotation the low Reynolds number approximation is made and the relative velocity between the particle and bubble can be modelled as outlined by Batchelor (1982) to give

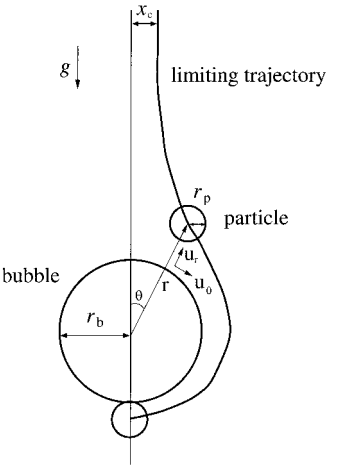

Figure 2 | Coordinate system used to model relative particle trajectories around the bubble.

$$u_r = L(U\cos\theta) - G\left(\frac{r_p + r_b}{6\pi\mu r_p r_b}\frac{d\Phi}{dr}\right) \tag{7}$$

$$u_\theta = M(U\sin\theta) \tag{8}$$

where u_r and u_θ are the relative radial and tangential velocities, respectively, of the particle moving around the bubble. It has been assumed that the bubble and particle are large enough ($r_p, r_b > 1$ μm) that the effects of Brownian motion can be ignored. As indicated in Figure 2, a polar coordinate system is used which is advected with the rising bubble with r measuring the distance from the centre of the bubble to the centre of the particle and θ measuring the upstream angle between the radius vector and the bubble axis parallel to the gravity vector. The bubble and particle are surrounded by water with density ϱ and dynamic viscosity μ. The relative approach speed of the bubble and particle at large separation distances is $U = U_p - U_b$ where U_p and U_b are the Stokes sedimenting velocities of the particle and bubble, respectively, given by $U_p = 2r_p^2(\varrho_p - \varrho)g/9\mu$ and $U_b = 2r_b^2(\varrho_b - \varrho)g/9\mu$ where ϱ_p and ϱ_b are the particle and bubble densities, respectively,

and g is the coefficient of gravity. The relative mobility functions for the bubble–particle interaction, L, G and M, depend on the bubble–particle separation distance and on the relative sizes and densities of the bubble and particle. The relative mobility functions can be calculated directly from the results presented by Jeffrey & Onishi (1984). The potential of the interparticle force is Φ where $\Phi = \Phi_{\mathrm{vdW}} + \Phi_{\mathrm{elec}}$ is the sum of the interparticle potentials due to van der Waals forces and electrostatic forces. Following Wang *et al.* (1997), Φ_{vdW} is calculated as

$$\Phi_{\mathrm{vdw}} = \frac{-A r_b r_p}{6(r_b + r_p)h}\left[1 - \frac{5.32h}{\lambda_{\mathrm{L}}}\ln\left(1 + \frac{\lambda_{\mathrm{L}}}{5.32h}\right)\right] \tag{9}$$

where A is the Hamaker constant for the bubble–particle interaction and h is the minimum separation distance between the bubble and the particle. As noted by Hunter (1987) A is typically of the order of 10^{-20} J for hydrosol systems. The London wavelength λ_L is typically assumed to by $\lambda_L = 0.1$ μm. The electrostatic force is modelled using

$$\Phi_{\mathrm{elec}} = -\frac{\varepsilon r_b r_p}{4(r_b + r_p)} \left(2\zeta_b\zeta_p \ln\left(\frac{1-\exp(-\varkappa h)}{1+\exp(-\varkappa h)}\right) + (\zeta_b^2 + \zeta_p^2)\ln(1-\exp(-2\varkappa h))\right) \tag{10}$$

where ε is the dielectric constant of water, ζ_p and ζ_b are the zeta potentials of the particle and bubble surfaces, respectively, and $\varkappa$ is the inverse Debye length which provides a measure of the electric double layer thickness. For a symmetric monovalent electrolyte an explicit formula can be written for the inverse Debye length:

$$\varkappa = \left(\frac{2e^2 c}{\varepsilon k T}\right)^{1/2} \tag{11}$$

where c is the electrolyte concentration, e is the magnitude of the charge on a single electron, k is Boltzmann's constant and T is temperature. In practice the influence of electrostatic forces during flotation are adjusted by adding coagulants which are absorbed on the particle and/or bubble surfaces in order to change the surface zeta potentials.

The mathematical model presented above has previously been used by others (Davis 1984; Melik & Fogler 1984; Nichols *et al.* 1995; Mazzolani *et al.* 1998) to study the gravity-induced coagulation of sedimenting solid spheres in the presence of van der Waals forces and/or electrostatic forces and by the current author (Leppinen 1999) to examine bubble–particle trajectories and collision efficiencies during microbubble flotation. Removal efficiencies are calculated using the mathematical model by numerically integrating Equations (7) and (8) in time in order to calculate the critical separation distance x_c indicated in Figure 2. The value of x_c is determined by integrating Equations (7) and (8) backwards in time along the trajectory which ends in particle capture at $\theta = \pi$ at the rear of the bubble (see Leppinen (1999) for details). Since time is only a parameter in Equations (7) and (8) it follows that relative trajectories cannot cross each other so that all trajectories which start inside of $x = x_c$ must result in particle capture.

The mathematical model presented above allows particle capture if the combined electrostatic and van der Waals forces are strong enough to overcome the hydrodynamic forces which result when fluid is drained from the gap between the particle and the bubble. An excellent review of some of the earlier studies which examine the combined effects of electrostatic, van der Waals and hydrodynamic forces is given by Derjaguin *et al.* (1981). These previous studies relied on simplified hydrodynamics which did not account for the influence of the particle on the motion of the bubble. By incorporating the two-sphere mobility functions L, G and M as defined in Jeffrey & Onishi (1984) into the current model it is possible to account for the exact hydrodynamics of the bubble–particle interaction. The model presented here assumes that the particle and bubble approach each other due to the force of gravity in an otherwise quiescent environment. This differs from the model of Matsui *et al.* (1998) and Fukushi *et al.* (1999) which accounts for bubble–particle collisions due to the combined influence of turbulent fluid motion and relative motion due to gravity. The key feature of the current model is the inclusion of interparticle forces which play a dominant role in determining flotation efficiency, yet are not included in the turbulent collision model of Matsui *et al.* (1998) and Fukushi *et al.*

(1999). The current model inherently assumes that, once a bubble becomes attached to a particle, then the probability of bubble detachment is zero. A more detailed discussion concerning the probability of bubble detachment is given by Derjaguin *et al.* (1981).

RESULTS

The effect of bubble and particle size

It is well known that successful flotation requires the use of coagulants to facilitate charge neutralisation of particles and to generate hydrophobic particles. There is less consensus, however, as to the optimal particle size for dissolved air flotation. Edzwald (1995) advocates the use of pin-point size flocs with d_p in the range of 10–30 μm which can be produced using relatively short flocculation times. Matsui *et al.* (1998) and Fukushi *et al.* (1999) argue that flotation rates are enhanced by increasing the size of the floc particles. The recommended larger flocs (with d_p as large as 1000 μm) require longer flocculation times and are subject to floc breakup in the contact zone of the flotation tank. The objective of this section is to use the mathematical model presented above to examine the influence of varying bubble and particle size on the rate of flotation.

The mathematical model presented in this paper can predict the removal rate of particles of size d_p, provided the physicochemical properties of the bubbles and particles are known. Throughout this paper the property values are chosen to be comparable with those reported in the experimental study of flotation reported in Okada *et al.* (1990). The property values employed are $\zeta_b = -40$ mV, $A = 3.4 \times 10^{-20}$ J, $\varkappa = 10^7$ m^{-1} and $\varrho_p = 1.05$ g cm^{-3}. The effect of particle charge neutralisation is examined in Figure 3 by comparing the case of electronegative particles with $\zeta_p = -40$ mV with the case of neutral particles with $\zeta_p = 0$ mV. Figure 3 shows the flotation rates R calculated using Equation (4) and the value of the collision efficiency E determined as a function of d_p and d_b from the mathematical model presented above. In order to make a valid comparison between the particle removal rates for different flotation parameters the rates are compared in terms of the fraction of particles removed with time for a fixed volumetric flux of air. Note that, if $\dot{V}''$ is the volumetric flux of air (i.e. the total volume of air injected per unit

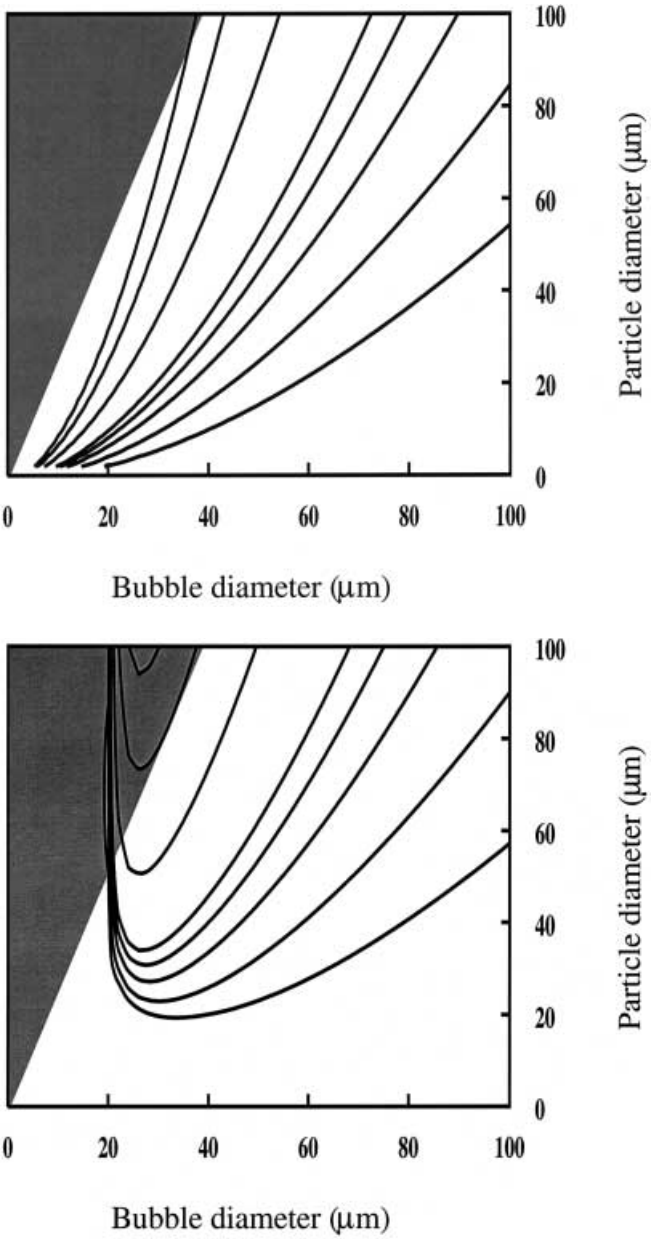

Figure 3 | Contour plots of flotation rate constant R for particles with $\zeta_p = -40$ mV (a) and $\zeta_p = 0$ mV (b). From the bottom right inwards the contour values are R=0.1, 0.25, 0.5, 0.75, 1.0, 2.5, 5.0, and 7.5 s^{-1}.

area of the control volume per unit time), then the number flux of bubbles is given by

$$\dot{n}_b'' = \frac{\dot{V}''}{\frac{4}{3}\pi r_b^3} \tag{12}$$

so that the number flux of bubbles depends inversely on the cube of the bubble radius. For all of the comparisons in this paper the volumetric flux of air has been held fixed at a rate of 1 cm^3 of air per m^2 per second.

Contour plots of the flotation rate as a function of bubble and particle diameter are plotted in Figure 3, with the case of strongly electronegative particles ($\zeta_p = -40$ mV) plotted in Figure 3(a) and the case of neutralised particles ($\zeta_p = 0$ mV) plotted in Figure 3(b). The contour lines in Figure 3 vary from $R = 0.1$ s^{-1} to $R = 7.5$ s^{-1}, as indicated in the figure caption. Only bubble–particle interactions to the right of the shaded regions result in the production of positively buoyant bubble–particle pairs. A comparison between Figures 3(a) and (b) shows the influence of particle charge neutralisation on flotation rates. The influence is relatively minor for the cases of relatively large bubbles and particles, however, for small bubbles and/or particles, the influence of charge neutralisation is dramatic. As seen in Figure 3(a) electrostatic forces can completely suppress dissolved air flotation when $d_p < 20$ μm and/or $d_b < 20$ μm. Figure 3(b) shows that, even in the case of particle charge neutralisation, flotation of small particles with $d_p < 10$ μm is relatively inefficient for bubbles typical of dissolved air flotation ($d_b \sim 40$ μm). The effective removal of these small particles either requires the use of very small bubbles ($d_b < 10$ μm) or it requires the particles to first flocculate to form larger particles. The overall conclusion from Figure 3 is that, if particle charge neutralisation can be achieved through the use of coagulants and the control of pH, then the flotation rate will be enhanced by increasing the particle sizes and decreasing the bubble sizes, subject to the constraint that the resulting bubble–particle agglomerates remain positively buoyant. If particle charge neutralisation cannot be achieved, there will be a minimum bubble size below which flotation is not possible.

The results presented in Figure 3 are meant to be illustrative of the effect of particle charge neutralisation and of the effect of varying bubble and particle sizes. A more thorough examination of the effect of varying the values of the physicochemical parameters of the system is presented by Leppinen (1999). The results presented in Figure 3 are generally supportive of the claim by Matsui *et al*. (1998) and Fukushi *et al*. (1999) that larger size flocs should be used to optimise flotation. This claim, however, must be treated cautiously. Successful flotation requires the formation of positively buoyant bubble–particle agglomerates. In the current model, which only allows for the attachment of a single bubble to each particle, the resultant bubble–particle agglomerates are only positively buoyant for bubble and particle sizes to the right of the shaded region in Figure 3. Flotation of particles within the shaded region of Figure 3 requires multiple bubble attachment and the modelling of this situation can be performed using the population balance approach adopted by Matsui *et al*. (1998) and Fukushi *et al*. (1999).

Polydisperse systems

The mathematical model presented in this paper can only be used directly to calculate particle removal rates if all of the particles and all of the bubbles are of a fixed size. This is because the value of the collision efficiency E varies as the particle and bubble sizes vary. In order to calculate the removal rates of particles when there is a distribution of bubble and particle sizes, a statistical approach is required. This paper incorporates a statistical model similar to that employed by Pan *et al*. (1996) in their global model of flotation efficiency. As shown in Figure 4, at time $t = 0$, n_p particles are randomly placed in a two-dimensional control volume, and bubbles are then randomly injected upwards through the control volume at a fixed rate in time. As each bubble passes through the control volume it interacts with the particles, and if the injection point of the bubble is such that a bubble–particle interaction leads to bubble–particle attachment, then that particular particle is removed from the control volume. It is assumed that a bubble can remove at most one particle and that each bubble acts independently. In particular, a given bubble is not injected until the preceding has passed through the control volume. Bubbles are repeatedly

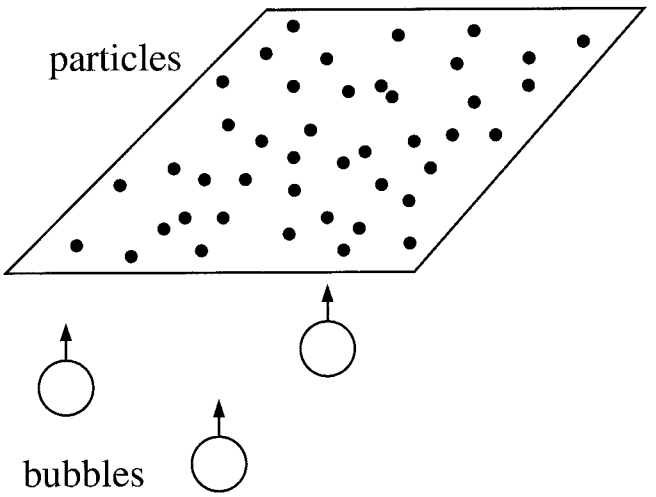

Figure 4 | Schematic of the random arrangement of particles and injection of bubbles used in the statistical model.

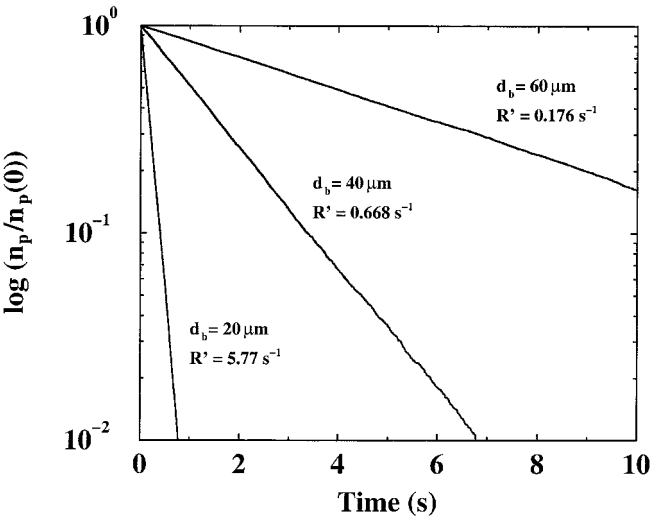

Figure 5 | Particle log fractions as a function of time for particles of size d_p=30 μm using bubbles of size d_b=20 μm, d_b=40 μm and d_b=60 μm.

injected until a specified fraction of particles have been removed, and each simulation is repeated many times to ensure that the removal rates are independent of the initial number of particles in the control volume. The distinction between the current statistical model and that employed by Pan *et al*. (1996) is that, in the current model, particle capture is determined by the removal efficiency E calculated using the mathematical model described above, whereas the particle capture criterion employed by Pan *et al*. (1996) is empirical in nature.

For the results presented here the statistical model is initialised by randomly locating 10,000 or more particles in a control volume measuring 10 cm by 10 cm. The objective is to determine the removal rate of particles as a function of time. All comparisons are made at a fixed volumetric flux of air of 1 cm^3 of air per m^2 of the control volume per second. By examining Equation (12) it is clear that the number flux of bubbles per unit time varies inversely with the cube of the size of the bubble.

As a test of the statistical model, removal rates of particles and bubbles of fixed size are calculated using property values of $\zeta_b = -40$ mV, $\zeta_p = -20$ mV, $A = 3.4 \times 10^{-20}$ J, $\varkappa = 10^7$ m^{-1} and $\varrho_p = 1.05$ g cm^{-3} which are comparable to those reported by Okada *et al*. (1990). Figure 5 compares the removal rates of particles of diameter $d_p = 30$ μm by three separate sizes of bubbles with $d_b = 20$ μm, 40 μm and 60 μm. Plotted in Figure 5 is the log of the particle fraction ($\log(n_p/n_p(0))$ as a function of time. In all cases the data lies upon a straight line with the slope of the line given by $-R'$. The successful implementation of the statistical model is verified by noting that the values of R' determined from Figure 5 differ by less than 1% from the value of the rate constant R calculated directly using Equation (4). For bubbles of diameter $d_b = 20$ μm the rate constant is $R' = 5.77$ s^{-1} while for bubbles of diameters $d_b = 40$ μm and $d_b = 60$ μm the rate constant is $R' = 0.668$ s^{-1} and $R' = 0.176$ s^{-1}, respectively. For the flotation parameters considered in Figure 5, the flotation rate constant strongly increases with decreasing bubble size, primarily due to the increase in the number flux of bubbles at a fixed total volumetric flux of bubbles. A physically more realistic application of the statistical model is to examine the removal rates of a distribution of particles of varying sizes by a distribution of bubbles of varying sizes. For example, consider the particle distribution given in Figure 6(a) with 5,000 particles varying in size from 4–12 μm and 15,000 particles varying in size from 20–40 μm. The smaller particles are typical of the size of some algae while the larger size range overlaps with the size range of 10–30 μm advocated by Edzwald (1995) for optimal flotation. The bubbles vary in size from

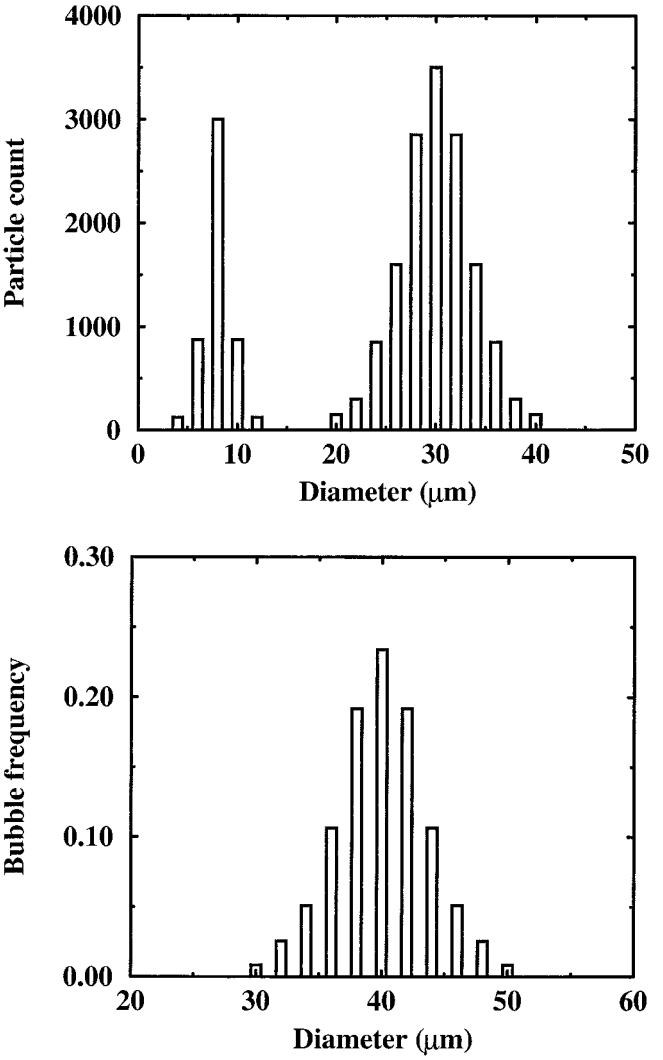

Figure 6 | Particle count (a) and bubble frequency (b) used to generate Figure 7.

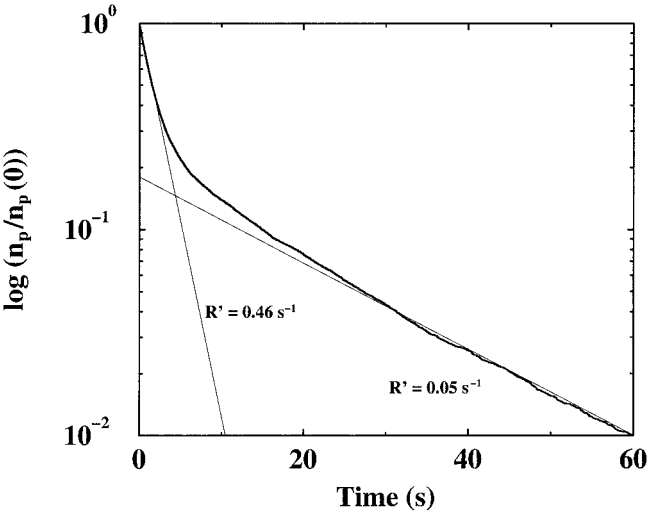

Figure 7 | Particle log fraction as a function of time for the bimodal particle distribution given in Figure 6 showing the asymptotic flotation rates at short and long times.

$d_b = 30$–50 μm with a mean of $d_b = 40$ μm as shown in Figure 6(b). The physical parameters for the bubbles and particles are the same as those used to generate the results in Figure 5. The particle removal rate is plotted in Figure 7 versus time where n_p is the sum of all of the particles over the full range of particle sizes. The key feature of Figure 7 is that the log removal rate of particles is clearly divided into a region with a high rate of particle removal at early times ($R' = 0.46$ s^{-1}) and a region with a lower removal rate at later times ($R' = 0.05$ s^{-1}). The current statistical model allows for the identification of the order in which the particles are removed, and during the early times in Figure 7, it is predominantly the larger particles which are removed, while at later times it is only the smaller, harder to float particles which remain. Based on batch flotation experiments, Ahmed & Jameson (1989) speculate that in some cases the flotation rate constant might be a function of time. The results in Figure 7 show that care is required when attempting to quantify flotation rate constants from the outcome of flotation batch test cell experiments. In most cases there will be a wide range of particles of differing sizes and/or differing surface chemistry and it may not be possible to identify a single flotation rate constant for a given experiment. For example, the identification of a period of fast particle removal followed by a period of low particle removal in the experimental results presented by Pan *et al.* (1996) may indicate the presence of two distinct particle types (either in terms of particle size, or particle surface chemistry) in the flotation test cell.

CONCLUSIONS

This paper has shown that it is possible to develop a kinetic model of dissolved air flotation without having to empirically assign an adhesion efficiency coefficient for

bubble–particle collisions. The model, however, does require the input of some physicochemical property values for the bubbles and particles. The mathematical model in this paper incorporates the exact hydrodynamics of the bubble–particle interaction including the influence of van der Waals and electrostatic forces. It is noted that bubble–particle attachment is only possible when the combined influence of van der Waals and electrostatic forces is stronger than the resistive hydrodynamic forces which result from attempting to squeeze water from the gap between the approaching bubble and particle.

If particle charge neutralisation can be achieved, flotation rates will be enhanced by decreasing the size of bubbles and increasing the size of particles. The increased flotation rate at small bubble sizes is primarily due to the increase in the number of bubbles released at a fixed volumetric gas flux. To date a limited control over the bubble size distribution generated in dissolved air flotation has been achieved by controlling the dissolved air saturator pressure, the recycle ratio and by using different injection nozzles (Rykaart & Haarhoff 1995; Vlašski *et al.* 1997). The results of this paper indicate that there is a large potential benefit from being able to control bubble size, and further study is warranted.

The results of this paper show that, while flotation is effective using the pin-point flocs advocated by Edzwald (1995) (10 μm$<d_p<$30 μm), the overall rate of flotation can be increased by increasing floc size. This conclusion however, must in turn be balanced with the need to produce positively buoyant bubble–particle agglomerates. If the particle size becomes too large, multiple bubble attachment, which is beyond the scope of the current paper, will be required for successful flotation. The specification of the optimal floc size therefore requires a compromise between the increased flotation removal rates of large particles versus the increased flocculation time (and ultimately increased size of the flocculation tank) required to produce the larger flocs and the need to produce positively buoyant bubble–particle agglomerates. Unless extremely small bubbles can be generated ($d_b<$10 μm) flocculation will be necessary for the efficient removal of very small particles ($d_p<$10 μm), even for cases of complete particle charge neutralisation.

ACKNOWLEDGEMENTS

The author acknowledges the financial support of Yorkshire Water plc and would like to thank Professor David Jeffrey for providing information concerning the calculation of the mobility functions L, M and G in Equations (7) and (8).

NOMENCLATURE

A	Hamaker constant
d_b (d_p)	bubble (particle) diameter
E	collision efficiency
g	coefficient of gravity
G, L, M	mobility functions
h	minimum separation distance between bubble and particle
n_p	particle number concentration per unit volume
$\dot{n}_b''$	bubble number flux per unit area
r	radial coordinate
r_b (r_p)	bubble (particle) radius
R	flotation rate constant
R'	flotation rate determined from stochastic model
t	time
u_r (u_θ)	radial (tangential) velocity
U	differential settling velocity between particle and bubble
U_b (U_p)	Stokes settling velocity of bubble (particle)
$\dot{V}''$	volumetric air flux per unit area
x_c	critical horizontal displacement for particle capture

Greek symbols

α_{pb}	adhesion efficiency
ε	dielectric constant of water
ζ_b (ζ_p)	bubble (particle) zeta potential
η_T	total single collector efficiency
θ	azimuthal angle
$\varkappa$	inverse Debye length

λ_L	London wavelength
μ	dynamic viscosity
ϱ	density of water
ϱ_b (ϱ_p)	density of bubble (particle)
Φ	total interparticle potential
Φ_{vdw}	van der Waals potential
Φ_{elec}	electrostatic potential

REFERENCES

Ahmed, N. & Jameson, G. J. 1989 Flotation kinetics. *Mineral Proc. Extract. Rev.* **5**, 77–99.

Batchelor, G. K. 1982 Sedimentation in a dilute polydisperse system of interacting spheres. Part 1. General theory. *J. Fluid Mech.* **119**, 279–408.

Bloom, F. & Heindel, T. J. 1997 A theoretical model of flotation de-inking efficiency. *J. Colloid Interface Sci.* **190**, 182–197.

Collins, G. L. & Jameson, G. J. 1976 Experiments on the flotation of fine particles. *Chem. Eng. Sci.* **31**, 985–991.

Collins, G. L. & Jameson, G. J. 1977 Double-layer effects in the flotation of fine particles. *Chem. Eng. Sci.* **32**, 239–246.

Davis R. H. 1984 The rate of coagulation of a dilute polydisperse system of sedimenting spheres. *J. Fluid Mech.* **145**, 179–199.

Derjaguin, B. V., Dukhin, S. S. & Rulyov N. N. 1981 Kinetic theory of flotation of small particles. *Surf. Colloid Sci.* **13**, 71–113.

Edzwald, J. K. 1995 Principles and applications of dissolved air flotation. *Wat. Sci. Technol.* **31**, 1–23.

Fukushi, K., Tambo, N. & Matsui, Y. 1995 A kinetic model for dissolved air flotation in water and wastewater treatment. *Wat. Sci. Technol.* **31**, 37–47.

Hunter, R. J. 1987 *Foundations of Colloid Science. Volume 1.* Clarendon Press, Oxford.

Jeffrey, D. J. & Onishi, Y. 1984 Calculation of the resistance and mobility functions for two unequal rigid spheres in low-Reynolds-number flow. *J. Fluid. Mech.* **139**, 261–290.

Leppinen, D. M. 1999 Trajectory analysis and collision efficiency during microbubble flotation. *J. Colloid Interface Sci.* **212**, 431–442.

Liers, S., Baeyens, J. & Mochtar, I. 1997 Modelling dissolved air flotation. *Wat. Env. Res.* **68**, 1061–1075.

Malley, J. P. & Edzwald, J. K. 1991 Concepts for dissolved air flotation treatment of drinking water. *J. Wat. Suppl.: Res. Technol.-AQUA* **40**, 7–17.

Matsui, Y., Fukushi, K. & Tambo, N. 1998 Modelling, simulation and operational parameters of dissolved air flotation. *J. Wat. Suppl.: Res. Technol.-AQUA* **47**, 9–20.

Mazzolani, G., Stolzenbach, K. D. & Elimelech, M. 1998 Gravity-induced coagulation of spherical particles of different size and density. *J. Colloid Interface Sci.* **197**, 334–347.

Melik, D. H. & Fogler H. S. 1984 Gravity-induced flocculation. *J. Colloid Interface Sci.* **101**, 73–82.

Nichols, S. C., Loewenberg, M. & Davis R. H. 1995 Electrophoretic particle aggregation. *J. Colloid Interface Sci.* **176**, 342–351.

Okada, K., Akagi, Y., Kogure, M. & Yoshioka, N. 1990 Analysis of particle trajectories of small particles in flotation when the particles and bubbles are both charged. *Can. J. Chem. Eng.* **68**, 614–621.

Pan, P., Paulsen, F. G., Johnson, D. A., Bousfield, D. W. & Thompson, E. V. 1996 A global model for predicting flotation efficiency Part 1: Model results and experimental studies. *TAPPI J.* **79**, 177–185.

Rykaart, E. M. & Haarhoff, J. 1993 Behaviour of air injection nozzles in dissolved air flotation. *Wat. Sci. Technol.* **31**, 24–36.

Vlašski, A. N., van Breemen, A. N. & Alaerts G. J. 1997 The role of particle size and density in dissolved air flotation and sedimentation. *Wat. Sci. Technol.* **36**, 177–189.

Wang, H., Zeng, S., Loewenberg, M. & Davis, R. H. 1997 Particle aggregation due to combined gravitational and electrophoretic motion. *J. Colloid Interface Sci.* **187**, 213–220.

Yoon, R. H. & Luttrell G. H. 1989 The effect of bubble size on fine particle flotation. *Mineral Proc. Extract. Metall. Rev.* **5**, 101–122.

Zabel, T. 1997 Flotation in water treatment. In *The Scientific Basis of Flotation*, pp. 349–377. Martinus Nijhoff.